Med Chem Res (2018) 27:520–530
DOI 10.1007/s00044-017-2078-4

MEDICINAL CHEMISTRY RESEARCH

ORIGINAL RESEARCH

Design, synthesis and biological evaluation of 2-Phenyl-4*H*-chromen-4-one derivatives as polyfunctional compounds against Alzheimer's disease

Manjinder Singh[1] · Maninder Kaur[1] · Bhawna Vyas[2] · Om Silakari[1]

Received: 1 June 2015 / Accepted: 15 September 2017 / Published online: 3 October 2017
© Springer Science+Business Media, LLC 2017

Abstract Polyfunctional compounds comprise a novel class of therapeutic agents for the treatment of multifactorial diseases. A series of 2-Phenyl-4*H*-chromen-4-one and its derivatives (**5a–n**) were designed, synthesized, and evaluated for their poly-functionality against acetylcholinestrase (AChE) and advanced glycation end products (AGEs) formation inhibitors against Alzheimer's disease (AD). The screening results showed that most of them exhibited a significant ability to inhibit AChE AGEs formation with additional radical scavenging activity. Especially, **5m**, **5b**, and **5j** displayed the greatest ability to inhibit AChE ($IC_{50} = 8.0$, 8.2, and 11.8 nM, respectively) and AGEs formation ($IC_{50} = 55$, 79, and 54 μM, respectively) with good antioxidant activity. Molecular docking studies explored the detailed interaction pattern with active, peripheral, and mid-gorge sites of AChE. These compounds, exhibiting such multiple pharmacological activities, can be further taken a lead for the development of potent drugs for the treatment of Alzheimer's disease.

Keywords AChE inhibitor · Alzheimer's disease · Antioxidants · Flavonoids · AGEs · Flavone

Abbreviations

ChE	Cholinesterase
AD	Alzheimer's disease
AChE	Acetylcholinesterase
AGEs	Advanced glycation end products
CAS	Catalytic active site
PAS	Peripheral anionic site
ACh	Acetylcholine
FDA	Food and drug administration
OS	Oxidative stress
ROS	Reactive oxygen species
Aβ	β-amyloid
RAGE	Receptor for AGEs
DPPH	1,1-diphenyl-2-picryl-hydrazyl
EWG	Electron withdrawing groups

Introduction

Alzheimer's disease (AD), a neurodegenerative disorder associated with a progressive loss of cognitive functions is emerging as one of the greatest health threat of the 21st century affecting almost 50% of adults over the age of 85 (Bishop et al. 2010). Several hypotheses that aim to explain the initiation and progression of the AD, including cholinergic hypothesis, amyloid hypothesis, tau hypothesis, calcium hypothesis, oxidative stress (OS) induction, advanced glycation end products (AGEs) induction, iron deregulation, mitochondrial dysfunction, etc., have been proposed. In the

Electronic supplementary material The online version of this article (https://doi.org/10.1007/s00044-017-2078-4) contains supplementary material, which is available to authorized users.

✉ Om Silakari
omsilakari@gmail.com

[1] Molecular Modeling Lab, Department of Pharmaceutical Sciences and Drug Research, Punjabi University, Patiala, Punjab 147002, India

[2] Department of Chemistry, Punjabi University, Patiala, Punjab 147002, India

light of various complex mechanisms and hallmarks involved in the pathogenesis of AD, it has been recognized as a complex neurodegenerative disorder with a multifaceted pathogenesis (Singh et al. 2016) (Fig. 1). Due to the pathological complexity, to date, no agent has proved to be considerably effective and the treatment options are limited for the clinicians. Thus, novel treatment strategy for AD is the biggest medical need for medical science and research.

The currently available anti-AD developed according to the reductionist paradigm of "one-molecule-one-target," has turned out to be palliative rather than curative. Thus, drug molecule that can act as multiple targets in neurotoxin cascades offers new hopes toward curing AD (Schmitt et al. 2004). Such multi-targeted agents can be developed with superior efficacy and safety profiles (Morphy and Rankovic 2005; Youdim and Buccafusco 2005).

Cholinergic hypothesis, which proposed that the extensive decrease of acetylcholine (ACh) leads to cognitive and memory deficits associated in AD patients represents one of the conventional hypothesis related to AD. Acetylcholinesterase (AChE) is the key enzyme for ACh hydrolysis at the cholinergic synapses, and therefore AChE inhibitors could increase the levels of ACh in AD patients through the inhibition AChE and thus relieve some symptoms experienced by AD patients (Singh et al. 2013). Till date, acetylcholinesterase inhibitors (AChEIs) are the only clinical used drugs for the treatment of AD (Fig. 2). Besides several diverse hallmarks AD brains display constant evidence of oxidative damage, which induces injury in the most cellular macromolecules of AD brain including nucleic acids, proteins, and lipids. These findings support the "OS hypotheses of AD," in which reactive oxygen species (ROS) play a key role in the onset and progression of AD (Markesbery 1997; Melo et al. 2003). Thus, drugs aimed at clearing or preventing the formation of the free radicals may be useful for the management of AD.

Moreover, the AGEs' (senescent macroprotein derivatives, formed through the non-enzymatic glycation called the "Maillard reaction") interact with a receptor for AGEs and provoke the generation of ROS and vascular inflammation, and consequently alters the various gene expressions in several types of cells, which could contribute to the

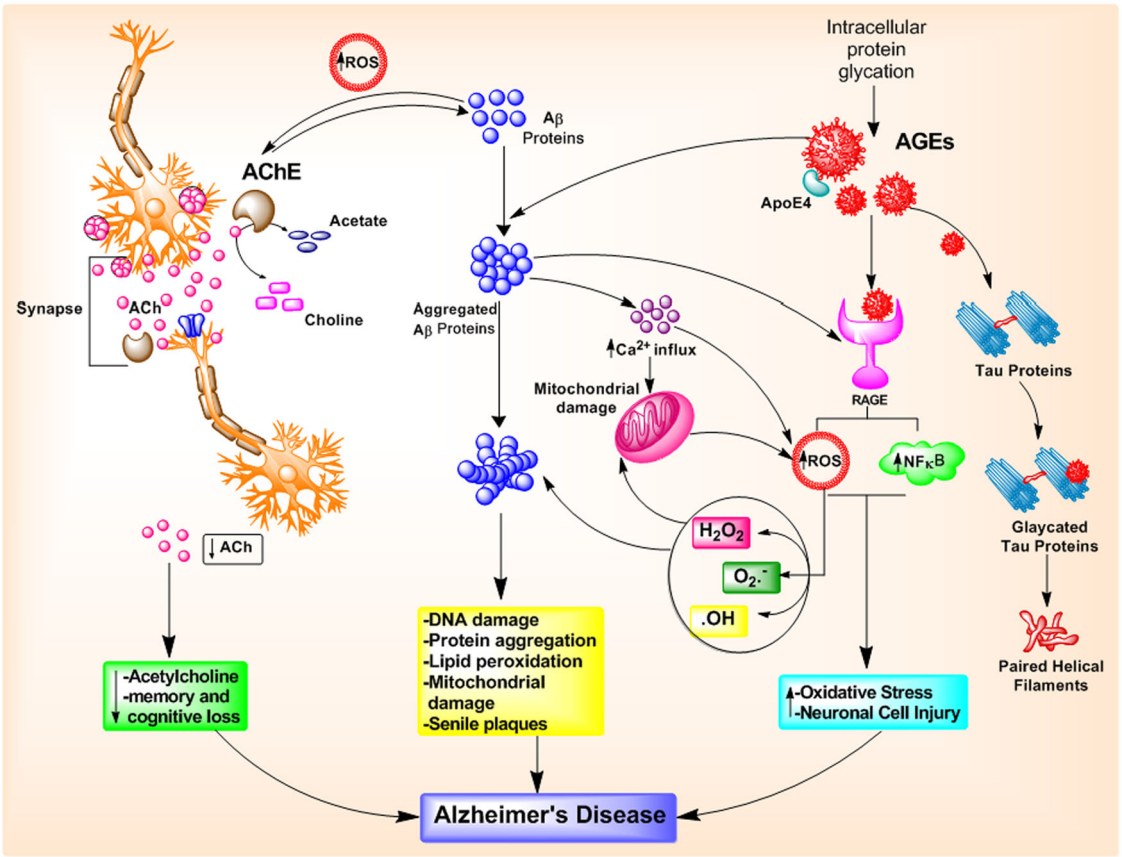

Fig. 1 Role of acetylcholinesterase, AGEs, and ROS in the pathophysiology of AD: AChE—acetylcholinesterase; ACh—acetylcholine; Aβ—β-amyloids; AGEs—advanced glycation end products; ApoE4—apolipoprotein E; RAGE—receptor for AGEs; ROS—reactive oxygen species;.OH—hydroxyl radicals; H_2O_2—hydrogen peroxide; $O_2^{\cdot-}$—superoxide anions; Ca^{2+}—calcium; NFκB—nuclear factor kappa-light-chain-enhancer of activated B cells

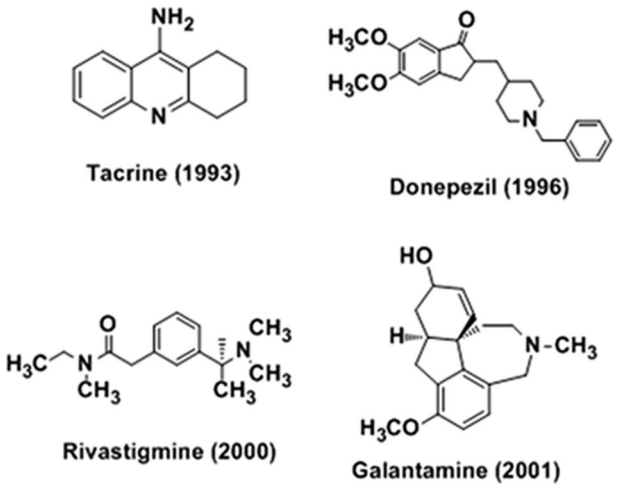

Fig. 2 FDA approved drugs for the treatment of Alzheimer's disease

pathological changes of AD as well (Munch et al. 1997; Yamagishi et al. 2003; Yan et al. 1994) (Fig. 1).

These interrelated hypotheses contribute to the complex pathogenesis of AD and the compounds that can act at different levels of the neurotoxic cascade or can modulate multiple targets simultaneously, offer new hopes toward curing AD. In the present study, flavone-based polyfunctional agents modulating ACh levels, having antioxidant potential along with AGEs formation inhibitory activity has been developed as novel therapeutics for the treatment of AD (Bolognesi et al. 2009).

Selection of appropriate privileged scaffold for designing of polyfunctional drug is a crucial step in the search of clinical candidates for the treatment of AD. Flavonoids having 2-Phenyl-4*H*-chrome-4-one scaffold are well-known natural compounds possessing a broad range of biological activities related to AD, such as neuroprotective effect (Lim et al. 2007), AChE inhibitory activity (Jung and Park 2007), Aβ fibril formation inhibitory activity (Kim et al. 2005), antioxidant properties (Zhu et al. 2007), AGEs formation inhibitory activity, etc. (Singh et al. 2014). Above-mentioned reports and natural antioxidant potential of flavonoids make them suitable scaffold for designing of polyfunctional drugs for the management of AD. In the present study, various derivatives were designed by exploring the different positions of ring-A and ring-B of 2-phenyl-4*H*-chromen-4-one scaffold to improve AChE and AGEs formation inhibitory activities with retention of radical scavenging effects. Thus, a series of polyfunctional flavone derivatives was synthesized in short steps and were tested for different biological activities. Moreover, the docking analysis was also employed to understand interactions of these derivatives with the active site of AChE.

Result and discussion

To develop a convincing drug candidate for multi-faceted AD, we commenced structure-based drug design approach considering 2-Phenyl-4*H*-chromen-4-one as a privileged scaffold, which has already been explored for its broad range of pharmacological properties for the management of AD. Although most of the synthesized derivatives have already been reported for various targets of other different disease conditions as anticancer, Tankyrases inhibitory, HSP90 receptor inhibitory, anti-mycobacterium, anti-anxiety, PGE_2 and COX-2 inhibtory, HIV-l integrase inhibitory activities, etc. (Lee et al. 2016; Cabrera et al. 2007; Cárdenas et al. 2006; Narwal et al. 2013; Lin et al. 2002; Dao et al. 2004; Fesen et al. 1994) none of these derivatives has been evaluated against targets of AD like AChE and AGEs formation. Moreover, till date, no 2-phenyl-4*H*-chrome-4-one scaffold-based poly-functional molecule for the management of AD has been reported to be used in clinical practice. Thus, it was thought worthwhile to consider this distinctive scaffold in poly-functional drug design program for AD.

Chemistry

The synthesis of the 2-Phenyl-4*H*-chromen-4-one derivatives **5(a–n)** was performed according to the Baker–Venkataraman rearrangement reaction with slight modifications depending on the stability and reactivity of the reagents used. The synthetic methodologies employed to develop intermediates (**3(a–n)**) and target compounds (**5 (a–n)**) are outlined in Scheme 1. The Baker–Venkataraman rearrangement is one of the fundamental reactions that involves conversion of *o*-hydroxyacetophenone into phenolic ester, which undergoes an intramolecular Claisen condensation in the presence of a base to form β-diketone (Baker 1933; Mahal and Venkataraman 1934). The compounds were dried, and then purified on silica columns using hexane:ethyl acetate (6:4) as solvent. The structures and purities of the target compounds were confirmed by IR, ^{1}H NMR, and mass analysis.

Evaluation of biological activity

1,1-Diphenyl-2-picryl-hydrazyl (DPPH) radical scavenging activity studies

All the compounds (**5a–n**) were tested for free radical scavenging activity by using DPPH assay at 517 nm. The DPPH scavenging activities of test compounds are summarized in Table 1. Most of the compounds (**5n**, **5l**, **5b**, **5k**, **5m**, **5h**, **5c**, **5i**, and **5j**) exhibited radical scavenging activity compared to ascorbic acid (Pi et al. 2008; Fang et al. 2008).

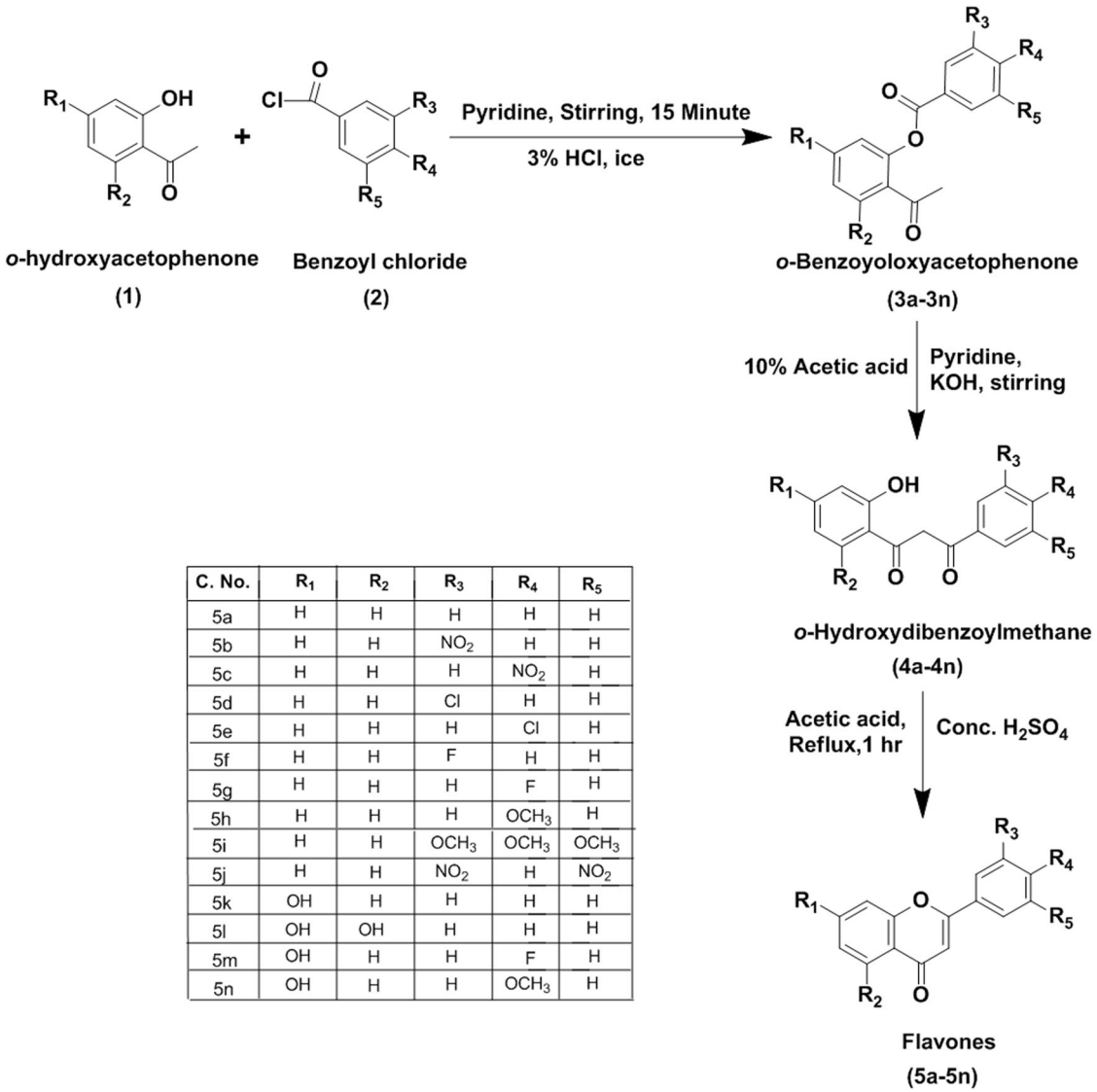

C. No.	R_1	R_2	R_3	R_4	R_5
5a	H	H	H	H	H
5b	H	H	NO_2	H	H
5c	H	H	H	NO_2	H
5d	H	H	Cl	H	H
5e	H	H	H	Cl	H
5f	H	H	F	H	H
5g	H	H	H	F	H
5h	H	H	H	OCH_3	H
5i	H	H	OCH_3	OCH_3	OCH_3
5j	H	H	NO_2	H	NO_2
5k	OH	H	H	H	H
5l	OH	OH	H	H	H
5m	OH	H	H	F	H
5n	OH	H	H	OCH_3	H

Scheme 1 Synthesis of 2-phenyl-4*H*-chromen-4-one derivatives (**5a–n**) with reagents and reaction conditions

Advanced glycation end-products formation inhibitory activity

All the synthesized compounds **5a–n** were subjected to in vitro AGEs formation inhibitory activity using the method reported by Matsuura et al. with slight modification (Matsuura et al. 2002). The potential of the compounds **5a–n** to inhibit AGEs formation is summarized in Table 1. All the synthesized compounds showed considerable AGEs formation inhibitory activity as the fluorescence of AGEs was shown to be remarkably reduced by all the synthesized compounds. Among the various synthesized compounds, **5l** ($IC_{50} = 33.0 \pm 1.91$ μM) was found to be 1.2 folds more potent than the standard drug aminoguanidine ($IC_{50} = 40.54 \pm 2.01$ μM). The compounds **5n**, **5k**, **5j**, **5m**, and **5i** (IC_{50} value ranging from 42.0 ± 1.82 to 58.0 ± 1.71 μM) also exhibited significant inhibitory activity. However, the compounds **5h, 5f**, **5b**, **5d**, **5a**, **5c**, **5g**, and **5e** (IC_{50} value ranging from 65.5 ± 0.52 to 148.5 ± 3.41 μM) exhibited lower anti-glycation activity as compared with the standard drug.

As evident from the results, among all the synthesized compounds, the compounds with hydroxyl substitution (**5k–5n**) were more active than the derivatives that lack hydroxyl group (**5a–5j**). Interestingly, di-hydroxyl-substituted derivative (**5l**) was found to be more active than the mono hydroxyl-substituted derivatives (**5n**, **5k**, and **5m**). Additionally, the derivatives with the electron releasing group at 7th position of ring-A showed higher activity (**5n**) than the derivatives with the electron withdrawing group at 7th position of ring-A (**5m**).

Moreover, the compounds having electron withdrawing groups (EWG) at the *meta* position of ring-B (**5f**, **5b**, and

Table 1 The AChE inhibition, DPPH radical scavenging activities and advanced glycation end products (AGEs) formation inhibitory activity of 2-phenyl-4*H*-chromen-4-one and derivatives (**5a–n**)

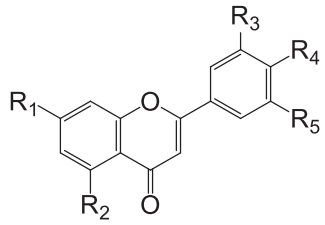

C. no.	R_1	R_2	R_3	R_4	R_5	AChE inhibitory activity (IC_{50}[b] ± SEM[a], nM)	Radical scavenging activity (IC_{50}[c] ± SEM[a], nM)	AGEs inhibitory activity (IC_{50}[d] ± SEM[a], μM)
5a	H	H	H	H	H	>100	100.0 ± 0.17	116.5 ± 0.71
5b	H	H	$-NO_2$	H	H	8.2 ± 0.31	24.5 ± 0.34	79.0 ± 1.32
5c	H	H	H	$-NO_2$	H	32.0 ± 0.23	29.0 ± 0.60	118.0 ± 0.85
5d	H	H	−Cl	H	H	31.0 ± 0.20	90.0 ± 0.65	91.0 ± 0.17
5e	H	H	H	−Cl	H	25.0 ± 0.90	82.5 ± 0.40	148.5 ± 3.41
5f	H	H	−F	H	H	37.0 ± 0.50	47.5 ± 0.52	77.0 ± 2.11
5g	H	H	H	−F	H	24.0 ± 0.50	47.0 ± 0.40	126.0 ± 0.17
5h	H	H	H	$-OCH_3$	H	16.0 ± 0.40	28.0 ± 0.28	65.5 ± 0.52
5i	H	H	$-OCH_3$	$-OCH_3$	$-OCH_3$	24.0 ± 0.28	30.0 ± 0.40	58.0 ± 1.71
5j	H	H	$-NO_2$	H	$-NO_2$	11.8 ± 0.24	31.0 ± 0.20	54.0 ± 2.13
5k	−OH	H	H	H	H	28.0 ± 0.20	25.0 ± 0.10	45.0 ± 2.11
5l	−OH	−OH	H	H	H	31.0 ± 0.57	23.5 ± 0.24	33.0 ± 1.91
5m	−OH	H	H	−F	H	8.0 ± 0.37	25.0 ± 0.15	55.0 ± 1.2
5n	−OH	H	H	$-OCH_3$	H	35.0 ± 0.84	20.5 ± 0.54	42.0 ± 1.82
Std.	Donepezil	–	–	–	–	12.7 ± 0.20	–	–
Std.	Ascorbic acid	–	–	–	–	–	20.0 ± 0.28	–
Std.	Aminoguanidine (AG)	–	–	–	–	–	–	40.54 ± 2.01

[a] SEM: Data are expressed as mean ± SEM ($n = 3$). Data were statistically analyzed by one-way ANOVA; $^*P < 0.05$ vs. Std

[b] IC_{50}, inhibitor concentration (means ± SEM of three experiments) for 50% inactivation of AChE

[c] IC_{50} was defined as the concentration resulting in 50% scavenging activity

[d] IC_{50} was defined as the concentration resulting in 50% inhibition of AGEs product formation

5d) showed high AGEs formation inhibitory activity as compared to compounds with EWG at the *para* position (**5c**, **5g**, and **5e**), as well as a compound with no substitution (**5a**). Besides, the electron releasing groups of ring-B (**5i** and **5h**) showed significant inhibitory potential than the compounds having electron withdrawing group (**5b–g**). Also, the *di*-nitro-substituted derivative (**5j**) showed better activity than mono nitro-substituted derivative (**5b** and **5c**). Thus, it can be concluded that flavone derivatives exhibited significant AGEs formation inhibitory activity that varies by different substitution patterns around the core structure.

In vitro AChE inhibition studies

The AChE inhibitory activity of all the synthesized compounds was tested in vitro, according to the modified Ellman's method (Ellman et al. 1961), using the rat brain homogenate, whereas donepezil was taken as a reference drug. The results are summarized in Table 1. Three independent experiments were performed to evaluate the AChE inhibitory effect of the synthesized compounds.

As shown in Table 1, among all, three compounds showed higher (**5m**, **5b**, and **5j**, $IC_{50} = 8.0$, 8.2 and 11.2 nM, respectively) AChE inhibitory activity than donepezil ($IC_{50} = 12.7$ nM). The compounds **5n**, **5g**, **5h**, and **5i** also showed significant AChE inhibitory activity. The compound **5m** with hydroxyl substituent at seventh position of ring-A and fluoro at the fourth position of ring-B showed highest AChE activity, i.e., IC_{50} 8.0 nM. Removal of the hydroxyl group resulted in 2–3 fold decrease in activity (**5h**, **5g**, and **5e**, $IC_{50} = 16.0$, 24.0, and 25.0 nM, respectively). Replacing of the electron withdrawing group of compound **5m** with an electron releasing group ($–OCH_3$) and introduction of a hydroxyl group at position seventh of ring A result in decrease activity (**5n**, $IC_{50} = 35.0$ nM). Also, compounds **5h** and **5i**, having a methoxy group at the ring-B showed significant AChE inhibitory potency ($IC_{50} = 16.0$ nM and 24.0 nM, respectively), indicating the importance of methoxy group in ring-B for AChE inhibition effects.

Additionally, it was observed that *meta*-substituted compounds (**5d** and **5f**, $IC_{50} = 31.0$ and 37.0 nM, respectively) showed less AChE inhibitory activity as compared to *para*-substituted compounds (**5g** and **5e**, $IC_{50} = 24.0$ and 25.0 nM, respectively), except *meta*-nitro-substituted derivative (**5b**, $IC_{50} = 8.2$ nM) that showed 4-fold higher activity as compared to *para*-nitro-substituted derivative **5c** ($IC_{50} = 32.0$ nM). This exception may be due to the reason that compound **5b** showed π–π stacking interaction with the conserved residue Trp279, major binding component of peripheral anionic site (PAS) and important interaction with Phe330, Phe288, and Arg289 of catalytic anionic site (CAS). Also, di-nitro-substituted derivative (**5j**) showed good AChE activity with IC_{50} 11.8 nM, than mono *para*-nitro-substituted derivative (**5c**). The flavone derivatives with hydroxyl groups substituted at ring-A (**5k–5n**) showed good AChE activity along with strong radical scavenging properties.

Molecular docking studies

To investigate the binding patterns of synthesized 2-phenyl-4*H*-chromen-4-one derivatives in the active site of AChE enzyme, molecular docking studies were carried out for **5m**, **5b**, and **5j** that showed good anti-cholinesterase activity. These compounds showed good fit in the active site by interacting with both catalytic site and PAS simultaneously. In compound **5m**, the hydroxyl group substituted at seventh position of the ring A showed hydrogen bonding interaction with Ser200 amino acid residue and His440 amino acid residue of the catalytic triad. The His440 amino acid residue also showed π–π stacking with the ring A. Additionally, the "O" of the ring C showed hydrogen bonding interaction with the Tyr121 amino acid residue of the PAS (Fig. 3). In compound **5b**, ring C showed π–π stacking with Trp279 amino acid residue of PAS; ring A showed π–π stacking with Tyr334 amino acid residue of PAS and with the Phe330 amino acid residue of catalytic triad. In addition to π–π stacking, hydrogen bonding interaction was observed between the carbonyl "O" of ring C and Phe288 and Arg289 amino acid residues of catalytic triad. Also, the nitro group substituted at third position of ring B showed two hydrogen bonding interactions with the Tyr121 amino acid residue of PAS (Fig. 4). Similarly, in compound **5j**, ring A showed π–π stacking with His440 amino acid residue of catalytic triad. Additionally, it showed two hydrogen bonding interactions, one between the "O" of ring-C and Tyr121 amino acid residue of PAS, and another between "O" of nitro group and Phe288 amino acid residue of catalytic triad (Fig. 5).

As evident from docking analysis, the compounds showed hydrogen bond, π–π (aromatic) and hydrophobic interactions with both CAS and PAS of AChE concurrently.

Conclusion

In the present study, 2-Phenyl-4*H*-chromen-4-ones derivatives have been developed as potential poly-functional anti-Alzheimer's agents. Most of the synthesized compounds exhibited potent AChE inhibitory activity with good radical scavenging and AGEs product formation inhibitory activity. The compounds **5m**, **5b**, and **5j** ($IC_{50} = 8.0$, 8.2, and 11.8 nM, respectively) displayed higher potency for AChE inhibition. Furthermore, molecular modeling study indicated that compounds **5m**, **5b**, and **5j** simultaneously bind with both CAS and PAS of the active site gorge. Additionally, these compounds had significant capacity to absorb free radicals and inhibit the AGEs formation. Thus,

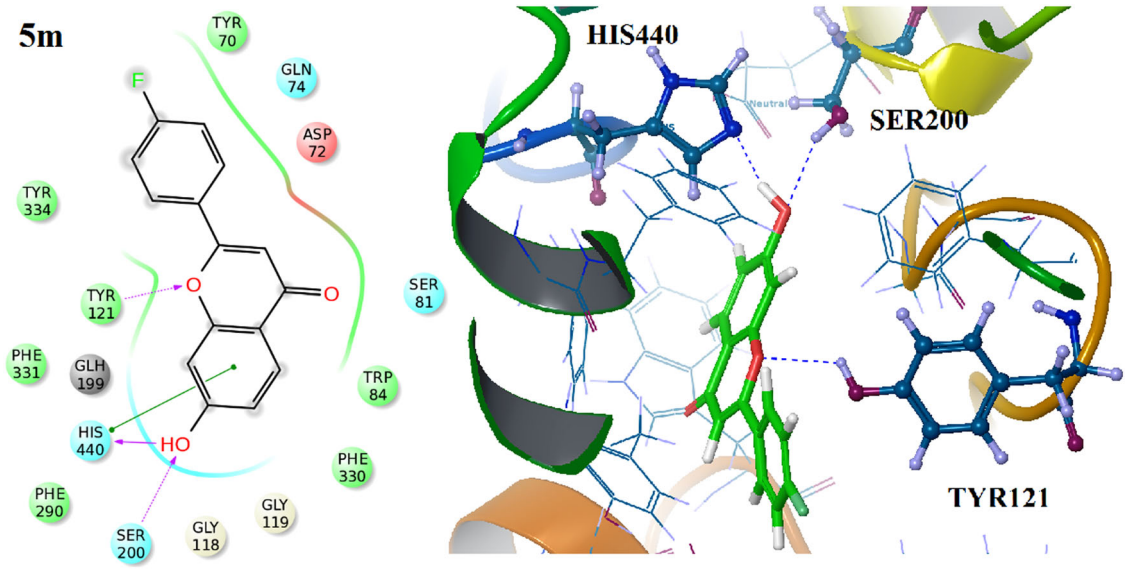

Fig. 3 Docked pose of interactions of flavone derivative (**5m**) with AChE (1EVE)

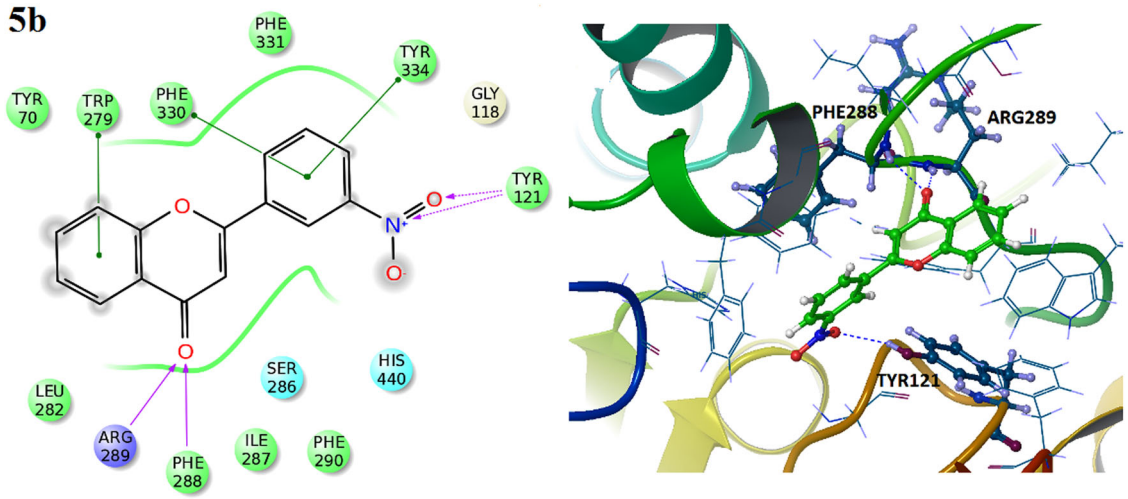

Fig. 4 Docked pose of interactions of flavone derivative (**5b**) with AChE (1EVE)

compounds **5m**, **5j**, **5l**, and **5n** have been found to be maximally potent polyfunctional molecules. These polyfunctional attribute of the 2-Phenyl-4*H*-chromen-4-ones make them potential candidates for the development of drugs for AD. However, further detailed investigations of mechanisms involved in these activities may establish their specific therapeutic usefulness.

Experimental section

Chemistry

All chemicals were procured from Sigma Aldrich Co., SD fine, Loba chemicals and were 99% pure, thus used without any purification. The completion of each reaction was monitored by thin layer chromatography (DC-Alufolien (20 × 20 cm) Kieselgel 60 F254 chromato plates) using hexane:ethylacetate (6:4) as a TLC development solvent system. All final compounds were purified on silica columns while all intermediates were purified by recrystallization from appropriate solvent. The melting point were recorded on a Labtronics digital automatic melting point apparatus and uncorrected, IR spectra were recorded on a Bruker (Alpha E) FT/IR spectrophotometer, ^{1}H-NMR spectra were recorded on a Bruker Advance II 400 MHz NMR spectrometer using chloroform ($CDCl_3$) or dimethylsulfoxide (DMSO-d_6) as solvent and tetramethylsilane (TMS) as an internal standard. Proton chemical shifts are expressed in parts per million (ppm). Mass spectra

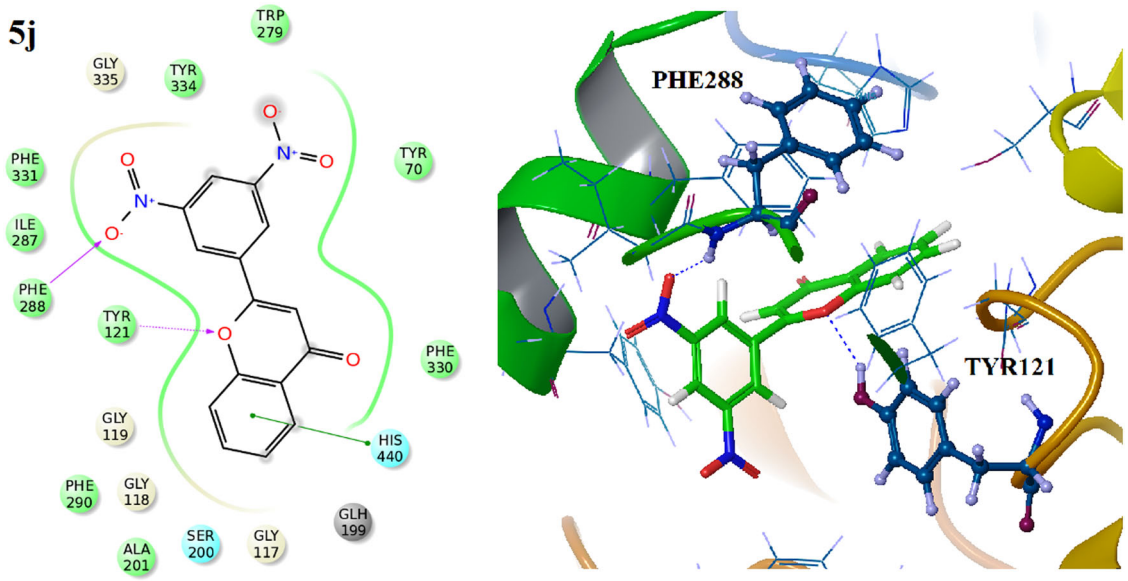

Fig. 5 Docked pose of interactions of flavone derivative (**5j**) with AChE (1EVE)

(ESI-MS, positive) were recorded with a Waters, Q-TOF micromass (LC-MS).

o-*Benzoyloxyacetophenones (**3a–n**)*

At first, the substituted *o*-benzoyloxyacetophenones (**3a–n**) were synthesized by stirring the mixture of substituted *o*-hydroxyacetophenone (0.1 mol) and substituted benzoyl chloride (0.15 mol) in dry pyridine. During the reaction, the mixture evolved spontaneous heat, and after about 15 min when the temperature comes down to room temperature, the mixture was poured with constant stirring into 3% hydrochloric acid containing crushed ice resulting in the precipitation of solid residue. The solid residue was then filtered and washed with methanol followed by water. The filtered residue was air dried and re-crystallized from methanol resulting in the white precipitates of substituted *o*-benzoyloxyacetophenone, yield 90%.

o-*Hydroxydibenzoylmethane (**4a–n**)*

To a warm solution of substituted *o*-benzoyloxyacetophenone (**3a–n**) in dry pyridine, hot pulverized 85% potassium hydroxide was added followed by mechanical stirring for 15 min resulting in the gradual appearance of yellow precipitates of potassium salt of substituted *o*-hydroxydibenzoylmethane (**4a–n**). The reaction mixture was brought down to room temperature and subsequently acidified with 100 mL of 10% acetic acid to desalt the compounds. The light-yellow precipitates of diketone (**4a–n**) were filtered and dried, yield 85%.

*2-Phenyl-4*H*-chromen-4-one derivatives (**5a–n**)*

The diketones (**4a–n**), in the presence of glacial acetic acid and concentrated sulfuric acid, were refluxed in water bath for 1 h, to achieve their cyclized products. Then, the reaction mixture was poured onto crushed ice with vigorous stirring, resulting in the precipitation of the 2-phenyl-4*H*-chromen-4-one and its derivatives. The product was filtered, thoroughly washed with water to make it free from acid and dried. Then, final compounds (**5a–n**) were purified on silica columns using hexane:ethyl acetate (6:4) as solvent.

2-Phenyl-4H-chromen-4-one (**5a**) White, crystalline, yield 91%, m.p.: 93–96 °C (reported 96–97 °C); ^{1}H-NMR (400 MHz, DMSO-d_6, δ ppm): 6.88 (1H, s), 7.48 (1H, m), 7.55–7.59 (3H, m), 7.68 (1H, d, $J = 8.24$ Hz), 7.75–7.80 (1H, m), 8.01 (2H, m) 8.13 (1H, dd, $J = 1.68$, 7.96 Hz). IR: (C=O) 1645 cm^{-1} (s), (C–O) 1375–1128 cm^{-1}. MS (ESI) $m/z = 223.07$ $[M+H]^+$, R_f value: 0.51 (hexane:ethyl acetate, 6:4).

2-(3-Nitrophenyl)-4H-chromen-4-one (**5b**) Light yellow, crystalline solid, yield 90%, m.p.: 251–256 °C; ^{1}H-NMR (400 MHz, $CDCl_3$, δ ppm): 6.92 (1H, s), 7.46–7.50 (1H, m), 774–7.78 (2H, m), 7.66 (1H, d, $J = 7.76$ Hz), 8.24–8.27 (2H, dd, $J = 1.80$, 7.76 Hz), 8.40 (1H, t, $J = 2.28$ Hz), 8.83 (1H, t, $J = 3.68$ Hz), IR: (C=O) 1631.49 cm^{-1} (m), (N=O) 1516, 1372 cm^{-1} (w), (C–O) 1363–1006 cm^{-1}. MS (ESI) $m/z = 268.07$ $[M+H]^+$, R_f value: 0.36 (hexane:ethyl acetate, 6:4).

2-(4-Nitrophenyl)-4H-chromen-4-one (**5c**) Dark gray, amorphous powder, yield: 86%, m.p.: 294–297 °C. 1H-NMR (400 MHz, DMSO-d6, δ ppm): 6.85 (1H, s), 7.43 (1H, m), 7.55 (2H, d, $J = 8.12$ Hz), 7.71 (1H, m), 8.05 (2H, dt, $J = 2.36$, 8.92 Hz), 8.18 (2H, dd, $J = 1.96$, 7.96 Hz), 8.20 (1H, m). IR (KBr pellets): (N=O) 1341, 1518 cm^{-1} (s), (C=C) 1601 cm^{-1} (m), (C=O) 1656 cm^{-1} (s), MS (ESI) $m/z = 268$ $[M+H]^+$, R_f value: 0.71 (hexane:ethyl acetate, 6:4).

2-(3-Chlorophenyl)-4H-chromen-4-one (**5d**) Light yellowish brown, amorphous powder, yield 83%, m.p.: 221–227 °C; ^{1}H-NMR (400 MHz, $CDCl_3$, δ ppm): 6.82 (1H, s), 7.42–7.53 (3H, m), 7.60 (1H, d, $J = 8.16$ Hz), 7.75 (1H, m), 7.80 (1H, d, $J = 2.84$, 7.64 Hz), 7.93 (1H, t, $J = 3.60$ Hz), 8.22–8.25 (1H, dd, $J = 1.56$, 7.96 Hz). IR: (C=O) 1633 cm^{-1} (s), (C–Cl) 1092 cm^{-1} (w), (C–O) 1363–1006 cm^{-1}. MS (ESI) m/z = 257 $[M+H]^+$, R_f Value: 0.60 (hexane:ethyl acetate, 6:4).

2-(4-Chlorophenyl)-4H-chromen-4-one (**5e**) Off white, amorphous powder, yield: 70%, m.p.: 191–194 °C (reported 188–190 °C). ^{1}H-NMR (400 MHz, $CDCl_3$, δ ppm): 6.84 (1H, s), 7.44 (1H, m), 7.51 (2H, d, $J = 8.64$ Hz), 7.58 (1H, d, $J = 7.88$ Hz), 7.72 (1H, m), 7.88 (2H, d, $J = 8.68$ Hz) 8.03 (1H, dd $J = 1.96$, 6.72 Hz), 8.24 (1H, dd, $J = 1.56$, 7.92 Hz). IR (KBr pellets): (C–Cl) 752 cm^{-1}(s), (C=C) 1596 cm^{-1} (m), (C=O) 1655 cm^{-1} (s). MS (ESI) $m/z = 257$ $[M+H]^+$, 258 [M+2], R_f value: 0.77 (hexane:ethyl acetate, 6:4).

2-(3-Fluorophenyl)-4H-chromen-4-one (**5f**) Gray, amorphous powder, yield 78%, m.p.: 211–215 °C; ^{1}H-NMR (400 MHz, $CDCl_3$, δ ppm): 6.83 (1H, s), 6.90–6.93 (1H, dd, $J = 2.20$, 8.72 Hz), 6.98 (1H, d, $J = 2.16$ Hz) 7.33 (1H, m), 7.54–7.59 (2H, m), 7.75–7.79 (1H, dt, $J = 3.96$, 7.92 Hz), 7.83 (1H, d, $J = 7.88$ Hz), 7.92 (1H, d, $J = 8.72$ Hz), IR: (C=O) 1621 cm^{-1} (s), (C–F) 1250 cm^{-1} (s), (C–O) 1382–1001 cm^{-1} MS (ESI) $m/z = 241.08$ $[M+H]^+$, R_f value: 0.40 (hexane:ethyl acetate, 6:4).

2-(4-Fluorophenyl)-4H-chromen-4-one (**5g**) White, amorphous powder, yield: 82%, m.p.: 143–145 °C (reported 148–150 °C). ^{1}H-NMR (400 MHz, $CDCl_3$, δ ppm):6.78 (1H, s), 7.26 (2H, m), 7.46 (1H, m), 7.58 (1H, dd, $J = 0.92$, 9.16 Hz), 7.72 (1H, m), 7.93 (2H, m) 8.25 (1H, dd, $J = 1.84$, 7.80 Hz). IR (KBr pellets): (C–F) 1039 cm^{-1} (w), (C=C) 1601 cm^{-1} (s), (C=O) 1657 cm^{-1} (s), MS (ESI) $m/z = 241$ $[M+H]^+$, R_f value: 0.54 (hexane:ethyl acetate, 6:4).

2-(4-Methoxyphenyl)-4H-chromen-4-one (**5h**) Light yellow, solid amorphous, yield 88%, m.p.: 155–158 °C (reported 154–156 °C); ^{1}H-NMR (400 MHz, $CDCl_3$, δ ppm): 3.90 (3H, s, $–CH_3$), 6.86 (1H, s), 7.03–7.05 (2H, dd, $J = 2.08$, 6.88 Hz), 7.43–7.45 (1H, dd, $J = 1.04$, 7.16 Hz), 7.58 (1H, dd, $J = 0.68$, 8.36 Hz), 7.69–7.71 (1H, m), 7.90–7.92 (2H, dd, $J = 2.12$, 9.0 Hz), 8.23 (1H, dd, $J = 1.64$, 8.0 Hz), IR: (C=O) 1648 cm^{-1} (s), MS (ESI) $m/z = 253.1$ $[M+H]^+$, R_f value: 0.49 (hexane:ethyl acetate, 6:4).

2-(3,4,5-Trimethoxyphenyl)-4H-chromen-4-one (**5i**) Light gray, solid amorphous, yield 76%, m.p.: 165–168 °C; ^{1}H-NMR (400 MHz, $CDCl_3$, δ ppm): 3.91, (3H, s, $–CH_3$), 3.94 (6H, s, $–CH_3$), 6.80 (1H, s), 7.18 (2H, d, $J = 12.56$ Hz), 7.42–7.46 (1H, m), 7.61 (1H, d, $J = 7.84$ Hz), 7.70–7.72 (1H, m), 8.81 (1H, dd, $J = 1.64$, 7.96 Hz), IR: (C=O) 1651 cm^{-1} (s), MS (ESI) $m/z = 313.1$ $[M+H]^+$ R_f value: 0.55 (hexane:ethyl acetate, 6:4).

2-(3,5-Dinitrophenyl)-4H-chromen-4-one (**5j**) Yellowish brown, solid amorphous, yield 83%, m.p.: 241–246 °C; ^{1}H-NMR (400 MHz, DMSO-d_6, δ ppm): 7.41 (1H, s), 7.50–7.54 (1H, m), 7.81–7.85 (2H, m), 8.13 (1H, d, $J = 7.12$ Hz), 9.08 (1H, t, $J = 2.0$ Hz), 9.24 (2H, d, $J = 1.96$ Hz), IR: (C=O) 1650 cm^{-1} (s), MS (ESI) $m/z = 312.1$ $[M+H]^+$, R_f Value: 0.60 (hexane:ethyl acetate, 6:4).

7-Hydroxy-2-phenyl-4H-chromen-4-one (**5k**) White, crystalline solid, yield: 65%, m.p.: 242–246 °C (reported 245–247 °C). ^{1}H-NMR (400 MHz, DMSO-d_6, δ ppm): 6.76 (1H, s), 6.90 (1H, dd, $J = 2.20$, 8.68 Hz), 6.95 (1H, d, $J = 2.16$ Hz), 7.53–7.57 (3H, m), 7.91–7.99 (2H, m), 7.92 (1H, d, $J = 8.72$ Hz), 10.60 (1H, s). IR (KBr pellets): (C=C) 1604 cm^{-1} (m), (C=O) 1658 cm^{-1} (s), (O–H) 3470 cm^{-1} (w). MS: *m/z*: 239.10 [M+1], R_f value: 0.24 (hexane:ethyl acetate, 6:4).

5,7-Dihydroxy-2-phenyl-4H-chromen-4-one (**5l**) Light yellowish, amorphous powder, yield: 72%, m.p.: 288–290 °C (reported 284–289 °C). ^{1}H-NMR (400 MHz, DMSO-d_6, δ ppm): 6.21 (1H, s), 6.46 (1H, d, $J = 2.04$ Hz), 6.79 (1H, s), 7.52–7.59 (3H, m), 7.98 (2H, dd, $J = 1.44$, 7.48 Hz), 10.63 (1H, s), 12.75 (1H, brs).IR (KBr pellets): (C=C) 1598 cm^{-1} (m), (C=O) 1652 cm^{-1} (s), (O–H) 3470 cm^{-1} (w). MS: *m/z*: 255.10 $[M+1]^+$, R_f value: 0.53 (hexane:ethyl acetate, 6:4).

2-(4-Fluorophenyl)-7-hydroxy-4H-chromen-4-one (**5m**) Grayish brown, amorphous powder, yield 90%, m.p.: 253–256 °C; ^{1}H-NMR (400 MHz, $CDCl_3$, δ ppm): 6.81 (1H, s), 6.90 (1H, dd, $J = 2.24$, 8.68 Hz), 6.96 (1H, d, $J = 4.0$ Hz), 7.30–7.35 (2H, m), 7.90 (1H, d, $J = 8.72$ Hz), 8.06–8.10 (2H, m), 10.66 (1H, s, –OH). IR: (C=O) 1647 cm^{-1} (s), (C–F) 1226 cm^{-1} (m), (O–H) 3665 cm^{-1}. MS (ESI) $m/z = 257.1$ $[M+H]^+$, R_f value: 0.57 (hexane:ethyl acetate, 6:4).

7-Hydroxy-2-(4-methoxyphenyl)-4H-chromen-4-one (**5n**) Brown black, amorphous solid, yield 91%, m.p.: 231–236 °C; ^{1}H-NMR (400 MHz, DMSO-d_6, δ ppm): 3.87 (3H, s, –CH_3), 6.69 (1H, s), 6.87–6.90 (1H, dd, $J = 2.20$, 8.68 Hz), 6.94 (1H, d, $J = 2.16$ Hz), 7.05–7.08 (2H, d, $J = 2.96$ Hz), 7.89 (1H, d, $J = 8.68$ Hz), 7.94–7.96 (2H, dd, $J = 1.88$, 7.0 Hz), 10.62 (1H, s, –OH). IR: (C=O) 1652 cm^{-1} (s) (O–H) 3701 cm^{-1}, MS (ESI) $m/z = 269.1$ $[M+H]^+$, R_f value: 0.53 (hexane:ethyl acetate, 6:4).

Pharmacology and molecular docking

DPPH radical scavenging activity method

The stable 1, 1-Diphenyl-2-picryl hydrazyl radical (DPPH) was used for determination of free radical-scavenging activity of the test compounds. The 0.1 mM solution of DPPH in methanol (39.4 mg in 1000 ml) was freshly prepared. Different concentrations of test compounds were added to an equal volume of methanol solution of DPPH. After 30 min at room temperature, the absorbance was recorded at 517 nm. IC_{50} values denote the concentration of the sample, which is required to scavenge 50% of DPPH free radicals. IC_{50} value was determined from the plotted graph of scavenging activity against the different concentrations of test compounds. Ascorbic acid was applied as positive drug (Blois 1958).

In vitro advanced glycation end-product (AGEs) formation inhibitory activity

The assay for the ability of the flavone to inhibit the glucose-mediated protein glycation and the development of fluorescent AGEs was performed. Different concentrations of various compounds were prepared by dissolving in DMSO. Antiglycation assay was performed according to the methods reported by Matsuura and colleagues with slight modification. In all experiments, about 500 µl of bovine serum albumin (1 mg/ml final concentration) was incubated with 400 µl of glucose (500 mM) in the presence of 100 µl of test compounds, aminoguanidine or phosphate buffer saline as control buffer at different concentrations. The reaction was allowed to proceed at 60 °C for 24 h and thereafter reaction was stopped by adding 10 µl of 100% (w/v) trichloroacetic acid (TCA). Then the mixture was kept at 4 °C for 10 min before subjecting to centrifugation at 15,000 rpm. The precipitate was redissolved in 1 ml alkaline PBS (pH 10) and immediately quantified for the relative amount of glycated BSA based on fluorescence intensity by spectrofluorometer LS-55 (Perkin Elmer) at 370 nm (excitation) and 440 nm (emission). Aminoguanidine was used as a positive control. Percentage inhibition was calculated. All experiments were performed in triplicate (Prathapan et al. 2012).

In vitro inhibition studies on AChE

AChE inhibitory activity was measured by the spectrophotometric method with slight modification; rat cortex homogenate was used as the source of AChE. For assay of AChE inhibitory activity, a reaction mixture containing 100 µl acetylthiocholine iodide 0.075 M/l, 100 µl sodium phosphate buffer (0.1 M/l, pH 7.4), 20 µl homogenate or serum and different concentrations of test compounds 20 µl were incubated at 37 °C for 15 min. The reaction was terminated by adding 50 µl 3% sodium lauryl sulfate, then, 50 µl of 0.2% of 5,5′–dithio-bis-(2-nitrobenzoic acid) was added to produce the yellow anion of 5-thio-2-nitro-benzoic acid. The values of IC_{50} were calculated by UV spectroscopy from the absorbance changes at 450 nm. Donepezil was applied as positive drug. All samples were assayed in triplicate.

Molecular docking studies

Among all the synthesized derivatives, compounds showing good anti-cholinesterase activity was sketched and cleaned in maestro molecular modeling workspace followed by energy minimization in "*ligprep*" program of Schrödinger software using OPLS_2005 force field at pH of 7.4 (Ligprep 2011). The X-ray crystallographic structure of the AChE complex with donepezil (PDB code 1EVE) was obtained from the Protein Data Bank and optimized for docking analysis (Kryger et al. 1999). The optimization protocol includes the addition of hydrogen atoms, deletion of water molecules, completion of bond orders, assignment of hydrogen bonds, and complex minimization to RMSD of 0.20 Å using OPLS_2005 force field. The studied molecules were docked into the active site of the protein using extra precision (XP) docking mode of "*glide*" program (Glide 2010; Friesner et al. 2004).

Statistical analysis

Data were analyzed by one-way ANOVA followed by Newman–Keuls multiple comparison test. All statistical analyses were processed using GraphPad prism software (version-5.01). Statistical significance was accepted for *P*-values of <0.05.

Acknowledgements We acknowledge the financial support from the "Indian Council of Medical Research (ICMR)", New Delhi, for providing us Senior Research Fellowships (ICMR-SRF); Award nos. BIC/11(11)/2014 and BIC/11(02)/2013.

Compliance with ethical standards

Conflict of interest The authors declare that they have no competing interests.

References

Lee J, Yu J, Son SH, Heo J, Kim T, An JY, Inn KS, Kim NJ (2016) A versatile approach to flavones via a one-pot Pd(II)-catalyzed dehydrogenation/oxidative boron-Heck coupling sequence of chromanones. Org Biomol Chem 14:777–784

Cabrera M, Simoens M, Falchi G, Lavaggi ML, Piro OE, Castellano EE, Vidal A, Azqueta A, Monge A, de Ceráin AL, Sagrera G, Seoane G, Cerecetto H, González M (2007) Synthetic chalcones, flavanones, and flavones as antitumoral agents: biological evaluation and structure–activity relationships. Bioorg Med Chem 15:3356–3367

Cárdenas M, Marder M, Blank VC, Roguin LP (2006) Antitumor activity of some natural flavonoids and synthetic derivatives on various human and murine cancer cell lines. Bioorg Med Chem 14:2966–2971

Narwal M, Haikarainen T, Fallarero A, Vuorela PM, Lehtio L (2013) Screening and structural analysis of flavones inhibiting tankyrases. J Med Chem 56:3507–3517

Lin YM, Zhou Y, Flavin MT, Zhou LM, Nie W, Chen FC (2002) Chalcones and flavonoids as anti-tuberculosis agents. Bioorg Med Chem 10:2795–2802

Dao TT, Chi YS, Kim J, Kim HP, Kim S, Park H (2004) Synthesis and inhibitory activity against COX-2 catalyzed prostaglandin production of chrysin derivatives. Bioorg Med Chem Lett 14:1165–1167

Fesen MR, Pommier Y, Leteurtre F, Hiroguchi S, Yung J, Kohn KW (1994) Inhibition of HIV-1 Integrase by flavones, caffeic acid phenethyl ester (Cape) and related compounds. Biochem Pharmacol 48:595–608

Baker W (1933) Molecular rearrangement of some o-acyloxyacetophenones and the mechanism of the production of 3-acylchromones. J Chem Soc 10:1381–1389

Bishop NA, Lu T, Yankner BA (2010) Neural mechanisms of ageing and cognitive decline. Nature 464:529–535

Blois MS (1958) Antioxidant determinations by the use of a stable free radical. Nature 181:1199–1200

Bolognesi ML, Rosini M, Andrisano V, Bartolini M, Minarini A, Tumiatti V, Melchiorre C (2009) MTDL design strategy in the context of Alzheimer's disease: from lipocrine to memoquin and beyond. Curr Pharm Des 15:601–613

Ellman GL, Courtney KD, Valentino A, Featherstone RM (1961) A new and rapid colorimetric determination of acetylcholinesterase activity. Biochem Pharmacol 7:88–95

Fang L, Kraus B, Lehmann J, Heilmann J, Zhang Y, Decker M (2008) Design and synthesis of tacrine-ferulic acid hybrids as multipotent anti-Alzheimer drug candidates. Bioorg Med Chem Lett 18:2905–2909

Friesner RA, Banks JL, Murphy RB, Halgren TA, Klicic JJ, Mainz DT, Repasky MP, Knoll EH, Shelley M, Perry JK, Shaw DE, Francis P, Shenkin PS (2004) Glide: a new approach for rapid, accurate docking and scoring. 1. Method and assessment of docking accuracy. J Med Chem 47:1739–1749

Glide (2010) Version 5.6. Schrodinger LLC, New York

Jung M, Park M (2007) Acetylcholinesterase inhibition by flavonoids from Agrimonia pilosa. Molecules 12:2130–2139

Kim H, Park BS, Lee KG, Choi CY, Jang SS, Kim YH, Lee SE (2005) Effects of naturally occurring compounds on fibril formation and oxidative stress of beta-amyloid. J Agric Food Chem 53:8537–8541

Kryger G, Silman I, Sussman JL (1999) Structure of acetylcholinesterase complexed with E2020 (Aricept): implications for the design of new anti-Alzheimer drugs. Structure 7:297–307

Ligprep (2011) Version 2.5. Schrodinger LLC, New York

Lim SS, Han SM, Kim SY, Bae YS, Kang IJ (2007) Isolation of acetylcholinesterase inhibitors from the flowers of chrysanthemum indicum linne. Food Sci Biotech 16:265–269

Mahal HS, Venkataraman KJ (1934) Synthetical experiments in the chromone group. Part XIV. The action of sodamide on 1-acyloxy-2-acetonaphthones. J Chem Soc 56:1767–1769

Markesbery WR (1997) Oxidative stress hypothesis in Alzheimer's disease. Free Radic Biol Med 23:134–147

Matsuura N, Aradate T, Sasaki C, Kojima H, Ohara M, Hasegawa J, Ubukata M (2002) Screening system for the maillard reaction inhibitor from natural product extracts. J Health Sci 48:520–526

Melo JB, Agostinho P, Oliveira CR (2003) Involvement of oxidative stress in the enhancement of acetylcholinesterase activity induced by amyloid beta-peptide. Neurosci Res 45:117–127

Morphy R, Rankovic Z (2005) Designed multiple ligands. An emerging drug discovery paradigm. J Med Chem 48:6523–6543

Münch Gl, Thome J, Foley P, Schinzel R, Riederer P (1997) Advanced glycation endproducts in ageing and Alzheimer's disease. Brain Res Rev 23:134–143

Pi RB, Ye MZ, Cheng ZY, Liu PQ (2008) Univ Zhongshan (UZHO-C). Patent CN101284812-A, China

Prathapan A, Nampoothiri SV, Mini S, Raghu KG (2012) Antioxidant, antiglycation and inhibitory potential of Saraca ashoka flowers against the enzymes linked to type 2 diabetes and LDL oxidation. Eur Rev Med Pharmacol Sci 16:57–65

Schmitt B, Bernhardt T, Moeller HJ, Heuser I, Frolich L (2004) Combination therapy in Alzheimer's disease: a review of current evidence. CNS Drugs 18:827–844

Singh M, Kaur M, Kukreja H, Chugh R, Silakari O, Singh D (2013) Acetylcholinesterase inhibitors as Alzheimer therapy: from nerve toxins to neuroprotection. Eur J Med Chem 70:165–188

Singh M, Kaur M, Silakari O (2014) Flavones: an important scaffold for medicinal chemistry. Eur J Med Chem 84:206–239

Singh M, Kaur M, Chadha N, Silakari O (2016) Hybrids: a new paradigm to treat Alzheimer's disease. Mol Divers 20:271–297

Yan SD, Chen X, Schmidt AM, Brett J, Godman G, Zou YS, Scott CW, Caputo C, Frappier T, Smith MA (1994) Glycated tau protein in Alzheimer disease: a mechanism for induction of oxidant stress. Proc Natl Acad Sci USA 91:7787–7791

Yamagishi S, Takeuchi M, Inagaki Y, Nakamura K, Imaizumi T (2003) Role of advanced glycation end products (AGEs) and their receptor (RAGE) in the pathogenesis of diabetic microangiopathy. Int J Clin Pharmacol Res 23:129–134

Youdim MB, Buccafusco JJ (2005) Multi-functional drugs for various CNS targets in the treatment of neurodegenerative disorders. Trends Pharmacol Sci 26:27–35

Zhu JT, Choi RC, Chu GK, Cheung AW, Gao QT, Li J, Jiang ZY, Dong TT, Tsim KW (2007) Flavonoids possess neuroprotective effects on cultured pheochromocytoma PC12 cells: a comparison of different flavonoids in activating estrogenic effect and in preventing beta-amyloid-induced cell death. J Agric Food Chem 55:2438–2445